Molecular Cell, Vol. 5, 197–206, February, 2000, Copyright ©2000 by Cell Press

A Ligand-Induced Extracellular Cleavage Regulates γ-Secretase-like Proteolytic Activation of Notch1

Jeffrey S. Mumm,*† Eric H. Schroeter,† Meera T. Saxena,† Adam Griesemer,† Xiaolin Tian,† D. J. Pan,§ William J. Ray,‡ and Raphael Kopan*†‖
*Neuroscience Program
Division of Biology and Biomedical Sciences
†Department of Molecular Biology and Pharmacology
Department of Medicine
Division of Dermatology
‡Departments of Psychiatry and Genetics
Washington University School of Medicine
St. Louis, Missouri 63110
§Department of Physiology
University of Texas Southwestern Medical Center
Dallas, Texas 75235

Summary

γ-secretase-like proteolysis at site 3 (S3), within the transmembrane domain, releases the Notch intracellular domain (NICD) and activates CSL-mediated Notch signaling. S3 processing occurs only in response to ligand binding; however, the molecular basis of this regulation is unknown. Here we demonstrate that ligand binding facilitates cleavage at a novel site (S2), within the extracellular juxtamembrane region, which serves to release ectodomain repression of NICD production. Cleavage at S2 generates a transient intermediate peptide termed NEXT (Notch extracellular truncation). NEXT accumulates when NICD production is blocked by point mutations or γ-secretase inhibitors or by loss of presenilin 1, and inhibition of NEXT eliminates NICD production. Our data demonstrate that S2 cleavage is a ligand-regulated step in the proteolytic cascade leading to Notch activation.

Introduction

Notch is a large, highly conserved, transmembrane receptor involved in a variety of cell–cell signaling interactions essential for metazoan development (Greenwald, 1998; Lewis, 1998). Notch is activated upon binding to membrane-anchored ligands from the Delta/Serrate/Lag-2 (DSL) family (Weinmaster, 1997). In addition, Notch mutations have been implicated in a number of disease states including cancer and dementia (Gridley, 1997).

Recent reviews have implicated proteolytic processing in maturation and activation of Notch (Chan and Jan, 1998, 1999). Maturation of the Notch protein is mediated by a furin-like convertase within the secretory pathway; cleavage occurs at an extracellular site (site 1 or S1) after the recognition sequence RQRR (Kopan et al., 1996; Logeat et al., 1998). The resultant polypeptides associate as an intramolecular heterodimer that is thought to be the only form of the Notch receptor found on the cell surface (Blaumueller et al., 1997; Logeat et al., 1998). We have recently demonstrated that activation of Notch involves cleavage between Gly-1743 and Val-1744 (termed here site 3 or S3; Schroeter et al., 1998). S3 cleavage serves to release the Notch intracellular domain (NICD) from the membrane. NICD then translocates to the nucleus where it functions as a transcriptional activator in concert with CSL family members (CBF-1, Suppressor of hairless, Lag-1; Jarriault et al., 1995).

Genetic analyses have established that the extracellular juxtamembrane region of Notch, in the absence of ligand binding, plays an inhibitory role in signaling (Kimble et al., 1998). Intracellular Notch (N^{IC}) and membrane-tethered proteins, which delete nearly all of the extracellular domain (collectively referred to here as $N^{\Delta E}$), function as ligand-independent, constitutively active proteins in vivo and are transcriptionally active in cell culture (Greenwald, 1994; Weinmaster, 1997). However, N-terminal deletion constructs that retain additional extracellular elements, most notably the Lin-12/Notch repeat (LNR) region, are unable to rescue Notch deficiency in *Drosophila* (Lieber et al., 1993; Struhl and Adachi, 1998) and show dramatically reduced activity in cell culture (Kopan et al., 1996; Schroeter et al., 1998). In addition, a subset of ligand-independent, gain-of-function alleles of Notch in *C. elegans* and *Drosophila* harbor extracellular missense mutations clustered in the LNR and juxtamembrane regions. This led to the hypothesis that ligand binding serves to counteract an extracellular negative control region located between the LNR region and the transmembrane domain (Greenwald, 1994; Kimble et al., 1998). However, the molecular modifications that underlie Notch activation in response to ligand binding remain largely undefined.

Using a strategy of mimicking genetically defined activating mutations and comparing active and inactive Notch proteins at the biochemical level, we have begun to define the molecular mechanisms that regulate Notch receptor activation. The data presented here demonstrate the existence of an ectodomain shedding-like cleavage event (S2) associated with activating mutations in Notch and induced upon ligand binding. We have termed the resultant carboxyl product NEXT (Notch extracellular truncation). Peptide sequencing shows that S2 cleavage occurs between Ala-1710 and Val-1711 residues, approximately 12 amino acids outside the transmembrane domain. Thus, NEXT is a naturally occurring equivalent of constitutively active, membrane-tethered, $N^{\Delta E}$ proteins. Pulse-chase analysis has demonstrated that $N^{\Delta E}$ proteins undergo S3 processing and are converted to NICD (Schroeter et al., 1998). Consistent with this observation, we present evidence that production of NEXT and NICD is linked: NEXT is enriched by blocking NICD production via point mutation, γ-secretase inhibitors, and loss of *presenilin 1* (PS1), while inhibition of NEXT production eliminates NICD accumulation. An

‖To whom correspondence should be addressed (e-mail: kopan@molecool.wustl.edu).

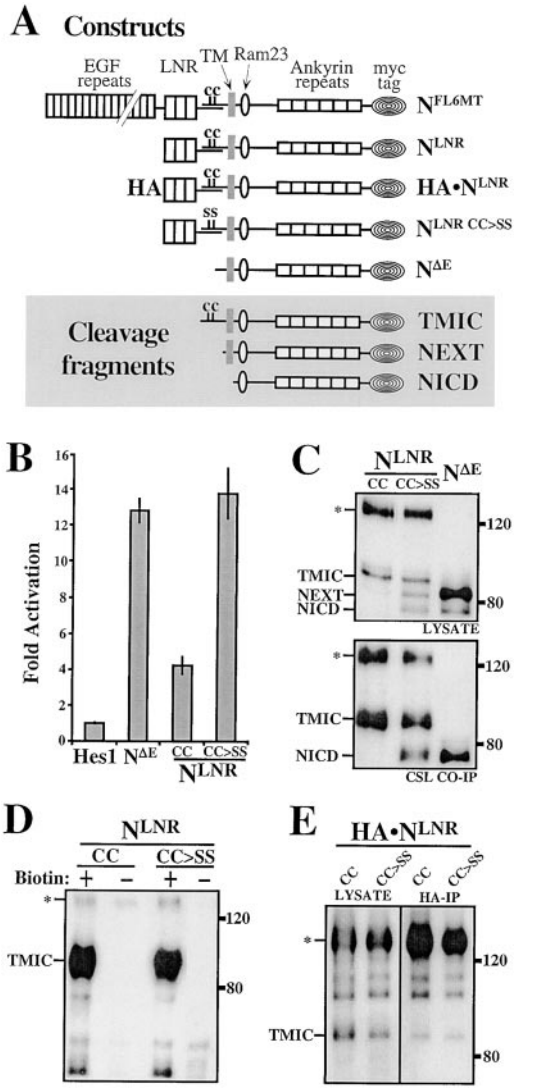

Figure 1. Activating Point Mutation Reveals NEXT Cleavage Fragment

(A) Schematic diagram of Notch constructs used. Note that all have the C-terminal 348 amino acids replaced by a hexameric myc tag to facilitate biochemical analysis. Conserved domains are labeled on top, also shown are the polypeptide products of S1, S2, and S3 cleavage, TMIC (termed also N^{TM}; Blaumueller et al., 1997), NEXT, and NICD, respectively (shaded box).

(B) Transactivation of Hes1-Luciferase demonstrates activity of $N^{LNR\ CC\rightarrow SS}$ equivalent to $N^{\Delta E}$. 3T3 cells were cotransfected with Hes1-Luciferase reporter, the indicated Notch construct, and β-gal as an internal control for transfection efficiency. Cells were lysed and luminescence evaluated 48 hr after transfection. Values shown are the average (±SD) of triplicate samples from a representative experiment.

(C) Robust transcriptional activity of $N^{LNR\ CC\rightarrow SS}$ correlates with NEXT (novel polypeptide, see text) and NICD processing. Anti-myc Western blot of anti-Flag coimmunoprecipitation (CSL CO-IP) and corresponding cell extract (LYSATE) is shown. HEK 293T cells were cotransfected with Flag-tagged $CSL^{RBP\text{-}J\kappa}$ and the indicated Notch construct. Cells were processed for anti-Flag CO-IP 48 hr after transfection. LYSATE and CSL CO-IP samples from cells transfected with $N^{\Delta E}$ are used as a marker for the relative position of NEXT and NICD. The asterisk indicates polypeptide prior to furin/S1 cleavage in Figures 2C–2E. Equivalent results were seen in 3T3, HeLa, and MEF cells.

initial inhibitor screen implicates metalloprotease activity in S2 proteolysis. In support of this, TACE (TNFα-converting enzyme) has been identified as a protease capable of S2 proteolysis in vitro (Brou et al., 2000 [this issue of *Molecular Cell*]). These data suggest that a ligand-induced proteolytic cascade activates Notch1; ligand binding serving to promote S2 cleavage, which is required for S3 cleavage.

Results

An Activating Mutation in Conserved Cysteine Residues Correlates with a Novel Extracellular Cleavage Event

Comparing the biochemical profile of activated mutant proteins to their parental constructs and to the wild-type receptor in the presence or absence of ligand, we hoped to gain insights into the regulation of Notch signaling. We first generated mouse Notch1 constructs in which two highly conserved cysteine residues (amino acids 1675 and 1682) have been mutated to serine, based on a *Drosophila* Notch construct that generates a hyperactive ligand-dependent receptor in vivo (Lieber et al., 1993). When tested for the ability to activate a Hes1-Luciferase reporter construct in tissue culture, a full-length version of this construct ($N^{FL\ CC\rightarrow SS\ 6MT}$) remained inactive (data not shown), possibly due to continued ligand dependence. However, we found that deletion of the EGF repeats ($N^{LNR\ CC\rightarrow SS}$) produced an activated, ligand-independent molecule (Figure 1B). To correlate $N^{LNR\ CC\rightarrow SS}$ transcriptional activity to S3 processing, Western blot analysis was performed. This analysis showed that the S1 carboxyl fragment ("TMIC" or p120; Figure 1A) was produced from both parental N^{LNR} and $N^{LNR\ CC\rightarrow SS}$ constructs and that S3 (NICD) cleavage occurs efficiently only for $N^{LNR\ CC\rightarrow SS}$ (Figure 1C). Surprisingly, a novel fragment was detected in extracts from cells transfected with $N^{LNR\ CC\rightarrow SS}$. This novel polypeptide migrates between the S1 and S3 products just below the unprocessed $N^{\Delta E}$ band, suggesting that it is the result of cleavage in the extracellular juxtamembrane region (Figure 1C). To determine the precise location of the cleavage site identified here, the unidentifed peptide was purified and N-terminally sequenced from a related, activated construct (see below and Figure 2). The sequence obtained, VKxEPVEP, matches only mouse Notch 1 in a nonstringent database search (BlastP). The

(D) Biotinylation of cell surface proteins indicates that the N^{LNR} and $N^{LNR\ CC\rightarrow SS}$ constructs are present at the cell surface. Anti-myc Western blot of streptavidin immunoprecipitation is shown. HEK 293T cells were transfected with N^{LNR} or $N^{LNR\ CC\rightarrow SS}$ constructs. Surface proteins were biotinylated 48 hr after transfection. The + biotin lanes of both constructs are greatly enriched for the TMIC fragment (compare to LNR lysate samples; e.g., Figure 2C).

(E) N-terminal (HA) immunoprecipitation shows that the postfurin intramolecular bond between Notch termini is unperturbed in N^{LNR} and $N^{LNR\ CC\rightarrow SS}$ constructs. Anti-myc Western blot of anti-HA immunoprecipitation (HA-IP) and corresponding cell extract (LYSATE) is shown. HEK 293T cells were transfected with $HA{\cdot}N^{LNR}$ or $HA{\cdot}LNR^{CC\rightarrow SS}$ constructs. Cells were processed for HA-IP 48 hr after transfection. The TMIC, C-terminal fragment is evident for both constructs following IP. The intermediate bands between unprocessed Notch and TMIC are unidentified polypeptides.

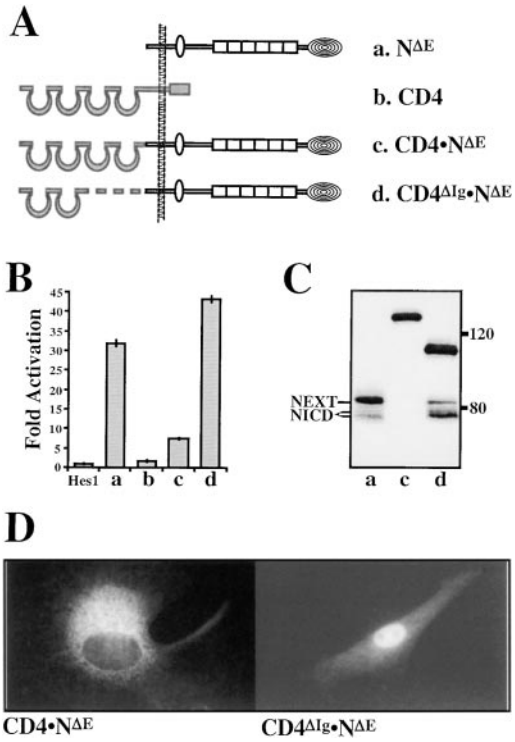

Figure 2. Active Chimeric Protein Undergoes NEXT and NICD Cleavage

(A) Diagram of CD4·Notch1 fusion proteins. Lowercase letters in (B) and (C) refer to constructs shown here. Note that these proteins lack the S1 site and thus do not undergo furin-mediated cleavage during maturation.

(B) Transactivation of Hes1-Luciferase demonstrates activity of CD4$^{\Delta Ig}$·N$^{\Delta E}$ equivalent to N$^{\Delta E}$. 3T3 fibroblasts were assayed as described in Figure 1B. Values shown are the average (±SD) of triplicate samples from a representative experiment.

(C) Robust transcriptional activity of CD4$^{\Delta Ig}$·N$^{\Delta E}$ correlates with NEXT and NICD cleavage. Anti-myc Western blot of lysates from 3T3 cells transfected with the indicated construct is shown. The NEXT and NICD fragments are evident for the active CD4$^{\Delta Ig}$·N$^{\Delta E}$ construct. Note that NICD appears as a doublet at this resolution, the upper band being a posttranslational modification of unknown significance (Schroeter et al., 1998).

(D) Subcellular localization detects nuclear translocation of the NICD fragment from a subset of CD4$^{\Delta Ig}$·N$^{\Delta E}$-expressing cells. 3T3 cells were transfected with the indicated construct. Cells were fixed in 4% paraformaldehyde (5 min) 48 hr after transfection, rinsed with PBS + 0.1% Triton-X100, washed with PBS, and then incubated with 9E10 anti-myc antibody. Cy3-conjugated goat anti-mouse secondary antibody was used for visualization. Nuclear staining of CD4·N$^{\Delta E}$ transfected cells has not been observed. Staining with Quantum Red–conjugated anti-human CD4 antibodies (Sigma) detects both molecules on the surface of live cells (data not shown).

novel polypeptide (NEXT) is thus generated as a result of proteolytic cleavage between amino acids Ala-1710 (−1) and Val-1711 (+1) within the extracellular domain, only 12 amino acids outside the transmembrane domain and 12 amino acids shorter than N$^{\Delta E}$ (Figure 1A and Figure 7). The novel cleavage site has been termed site 2 (S2) to delineate it from the furin-like cleavage (S1) and NICD producing cleavage (S3) sites. Interestingly, Notch is cleaved in vitro at this site by TACE, also known as ADAM 17 (a disintegrin and metalloprotease; Brou et al., 2000).

NICD and the vertebrate CSL protein, RBP-Jκ (CSL$^{RBP\text{-}J\kappa}$), are known to interact in the nucleus (Jarriault et al., 1995). Flag-tagged CSL$^{RBP\text{-}J\kappa}$ is localized predominantly within the nucleus of mammalian cells (J. S. M. and R. K., unpublished data). Thus, CSL coimmunoprecipitation (CSL CO-IP) serves to enrich for NICD fragments in cells transfected with active Notch and Flag-tagged CSL$^{RBP\text{-}J\kappa}$ (Schroeter et al., 1998). CSL CO-IP revealed substantial enrichment of NICD from N$^{LNR\ CC\rightarrow SS}$ with no appreciable NICD generation from N^{LNR} (Figure 1C, note that longer exposures reveal modest NEXT and NICD production from N^{LNR}, consistent with the low level of HES1 transactivation seen in Figure 1B). Presumably, NICD enrichment is due to colocalization of these proteins in the nucleus prior to lysis. However, postlysis associations are not totally eliminated under the conditions used here (J. S. M. and R. K., unpublished data), and other Notch fragments are also recovered (e.g., TMIC and unprocessed Notch; Figure 1C). Unlike NICD, which is always enriched in these preparations, other fragments (including NEXT) are recovered with variable efficiency.

NEXT could be a short-lived intermediate processed at the cell surface or produced intracellularly. In order to ensure that N$^{LNR\ CC\rightarrow SS}$ is properly secreted, biotinylation of cell surface proteins was performed. The C-terminal product of S1 cleavage (TMIC) was biotinylated, indicating that N$^{LNR\ CC\rightarrow SS}$ is present at the plasma membrane (Figure 1D). Additionally, immunoprecipitation of the N terminus (using N-terminally HA-tagged versions of N^{LNR} and N$^{LNR\ CC\rightarrow SS}$) verified that the C→S mutations do not disrupt intramolecular heterodimeric associations between termini following S1 cleavage; the C terminus was recovered from both constructs (Figure 1E). These results verify that the CC→SS mutation does not cause aberrant maturation and/or mistrafficking.

Other Activated Notch Constructs Produce NEXT and NICD

To determine if intramembranous proteolysis of Notch can be inhibited in the presence of sequences other than Notch at the extracellular surface, we fused the extracellular domain of CD4 to N$^{\Delta E}$ (CD4·N$^{\Delta E}$; Figure 2A). We also fused a truncated CD4 ectodomian to N$^{\Delta E}$ (CD4$^{\Delta Ig}$·N$^{\Delta E}$; Figure 2A), which may cause a modulation of the oligomerization state of CD4 proteins in fibroblasts (Sakihama et al., 1995). Since the CD4 ectodomain is not believed to undergo extracellular cleavage (Sadhukhan et al., 1998), these proteins allow us to test whether the juxtamembrane, transmembrane, and/or intracellular domain(s) of Notch are sufficient for protease recognition and cleavage.

CD4·N fusion proteins were tested for their ability to activate the Hes1-Luciferase reporter. The CD4·N$^{\Delta E}$ chimera is not active, establishing that heterologous ectodomains are capable of negatively regulating S3 cleavage. However, the shorter CD4$^{\Delta Ig}$·N$^{\Delta E}$ chimera is equivalent to N$^{\Delta E}$ controls in its ability to activate Hes1 (Figure 2B). Western blot analysis demonstrated that the active CD4$^{\Delta Ig}$·N$^{\Delta E}$ protein is processed, showing both NEXT and NICD production, while inactive constructs are not cleaved (Figure 2C). Anti-myc immunostaining detected nuclear localization of CD4$^{\Delta Ig}$·N$^{\Delta E}$ derived NICD

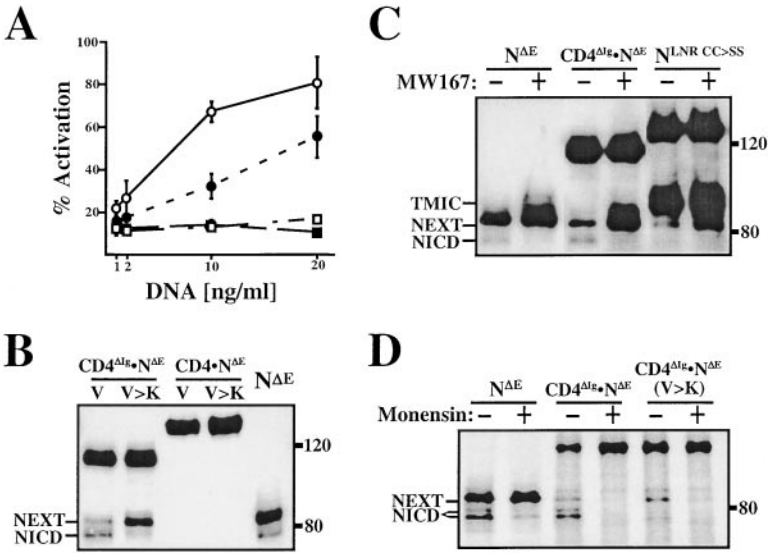

Figure 3. NEXT and NICD Form a Proteolytic Cascade

(A) Transactivation of Hes1-Luciferase demonstrates inhibition of activity by S3 point mutation (V1744K). Transfected Notch constructs were titrated (ng/ml of media) against constant reporter concentration as described previously (Schroeter et al., 1998). The circles indicate activity of CD4$^{\Delta lg}$·N$^{\Delta E}$; squares indicate activity of CD4·N$^{\Delta E}$. Open symbols are wild type; closed symbols indicate the V→K mutation. 3T3 fibroblasts were assayed as described in Figure 1B; transactivation is expressed as percent activity of 50 ng of ΔEMV (100% represents 11-fold activation in this experiment). Values shown are the average ± SD of triplicate samples from a representative experiment.

(B) NICD inhibition by S3 point mutation (V1744K) results in NEXT accumulation. Anti-myc Western blot of lysates from 3T3 cells transfected with the indicated construct is shown. Note intensification of NEXT band in the absence of S3 processing (CD4$^{\Delta lg}$·N$^{\Delta E}$).

(C) Prolonged inhibition of S3 processing by MW167 results in dramatic accumulation of the NEXT fragment. Anti-myc Western blot of lysates from HEK 293T cells transfected with the indicated construct is shown. Cells were treated (+) three times at 9 hr, 6 hr, and again at 3 hr prior to lysis, with 50 μM MW167 in DMSO. Control cells (−) recieved equivalent amounts of DMSO only.

(D) Inhibition of NEXT production, by monensin, indicates that S2 proteolysis, like S3, occurs post-Golgi. Autoradiograph of ^{35}S-labeled, anti-myc immunoprecipitated proteins from HEK 293T cells transfected with the indicated construct is shown. Cells were metabolically labeled with 50 μCi/ml [^{35}S]methionine in the presence or absence of 100 μM monensin 4 hr prior to lysis. Monensin-treated cells show inhibition of S2 processing results in a coincident inhibition of S3 processing. Efficacy of inhibition was confirmed by quantitation of band intensity.

fragments in a subset of transfected cells, while CD4·N$^{\Delta E}$ proteins were restricted to the cytoplasm (Figure 2D). Equivalent amounts of both CD4·Notch chimeric proteins were detected at the cell surface by labeling live cells with flourescently conjugated anti-CD4 antibodies (data not shown). This result confirms that the S2 protease recognition sequence is located C-terminally to the CD4$^{\Delta lg}$·N$^{\Delta E}$ fusion point (Ile-1704) and suggests that one role of the Notch extracellular domain is to negatively regulate this proteolytic step.

A Proteolytic Cascade Activates Notch Signaling

The correlation between S2 and S3 processing in activated Notch proteins raises the possibility that the two are linked in a proteolytic cascade. Using pulse-chase analysis, we have previously demonstrated that N$^{\Delta E}$, a NEXT-like protein, is completely converted to NICD in 10T1/2 cells (Schroeter et al., 1998). Therefore, one prediction of the cascade hypothesis is that NEXT will accumulate if its conversion to NICD is blocked. A single point mutation was introduced into CD4$^{\Delta lg}$·N$^{\Delta E}$ at the −1 position of the S3 site (V1744K, CD4$^{\Delta lg}$·N$^{\Delta E}$ V→K). This mutation reduces the rate of S3 cleavage and signaling activity of N$^{\Delta E}$ (Schroeter et al., 1998). Titration of this construct over a range of DNA concentrations revealed that S3 mutations also reduced the activity of CD4$^{\Delta lg}$·N$^{\Delta E}$ (Figure 3A), confirming the dependence of CD4$^{\Delta lg}$·N$^{\Delta E}$ activity on S3 processing. Furthermore, Western blots revealed that this point mutation, by inhibiting S3 cleavage, led to accumulation of the NEXT fragment (Figure 3B). Additionally, a previously described S3 protease inhibitor, MW167, inhibits NICD production from N$^{LNR\ CC\rightarrow SS}$ and CD4$^{\Delta lg}$·N$^{\Delta E}$. As shown in Figure 3C, high levels of NEXT accumulate, at the expense of NICD, after exposure to multiple doses of 50 μM MW167. Identical results were obtained with S3 protease inhibitors from several classes (J. S. M., E. H. S., and R. K., unpublished data). Similar accumulation of NEXT was also detected in cells deficient for PS1 (see below), presumably due to a previously demonstrated inhibition of S3 cleavage in these cells (De Strooper et al., 1999). These results are consistent with NEXT being a transient intermediate that undergoes S3 cleavage.

If NEXT is a signaling intermediate, then it should be processed prior to S3 cleavage. In order to more thoroughly define the cellular compartment where S2 cleavage occurs, we tested an exocytic pathway inhibitor, monensin, for the ability to abrogate S2 processing. Monensin disrupts transport from the *trans*-Golgi network to the cell surface and has previously been shown to inhibit S3 cleavage (Schroeter et al., 1998) but not S1 cleavage (Blaumueller et al., 1997). The results show that monensin is a strong inhibitor of S2 cleavage (Figure 3D). Interestingly, at the concentration tested, monensin reduces S3 cleavage by only 70% from N$^{\Delta E}$ (data not shown), yet no residual NICD product is evident from the CD4·N$^{\Delta E}$ chimeras. Collectively, these results are consistent with the proteolytic cascade hypothesis whereby NEXT is produced at the cell surface and subsequently converted to NICD, thus activating the Notch pathway.

A critical prediction of the cascade hypothesis is that S3 cleavage depends on the generation of NEXT. If S2 cleavage is required for S3 cleavage, then inhibition of NEXT processing should result in reduced NICD formation. An alternative, parallel pathway hypothesis predicts that NEXT and NICD are independently produced from an upstream precursor. This alternative model would predict that NICD would accumulate upon inhibition of NEXT. To test this, we screened a series of proteinase inhibitors for their ability to inhibit S2 cleavage

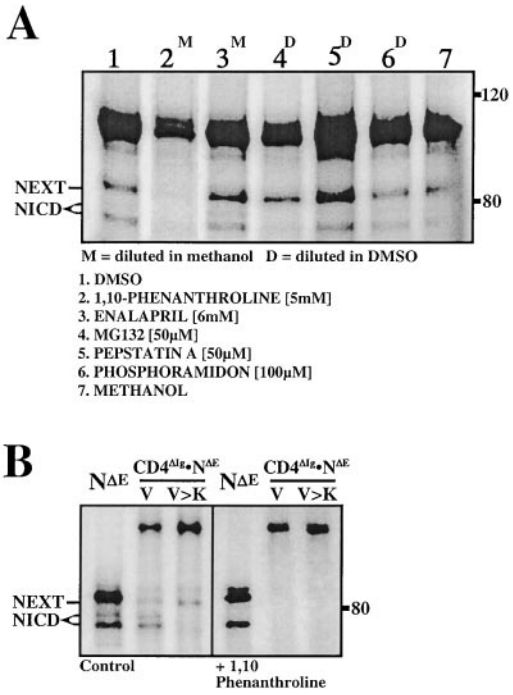

Figure 4. Metalloprotease Activity Implicated in S2 Proteolysis

(A) Inhibition of S2 processing, by the divalent chelator 1,10 o-phenanthroline (OP), implicates the metalloprotease family in S2 cleavage. Autoradiograph of ^{35}S-labeled, anti-myc immunoprecipitated proteins from HEK 293T cells transfected with CD4$^{\Delta lg}$·N$^{\Delta E}$ V→K is shown (the V→K point mutant was used to facilitate metabolic labeling of the NEXT fragment). Cells were metabolically labeled with 50 μCi/ml [^{35}S]methionine in the presence of the indicated reagent 4 hr prior to lysis. The panel of reagents included inhibitors of metalloproteases (both broad-spectrum, lane 2, and specific, lanes 3 and 6), γ-secretase and the proteosome (lane 4), and aspartyl proteases (lane 5). Efficacy of inhibition was confirmed by quantitation of band intensity. Other serine and cysteine protease inhibitors tested but not shown included aprotinin, leupeptine, and PMSF.

(B) NICD production is blocked by inhibition of S2 processing suggesting that NEXT is a precursor of NICD. Autoradiograph of ^{35}S-labeled, anti-myc immunoprecipitated proteins from HEK 293T cells transfected with the indicated construct and processed in the presence of 5 mM OP as in (A) above. Control cells received equivalent amounts of methanol. N$^{\Delta E}$ lanes shows that S3 cleavage is not inhibited directly by OP, thus confirming that S2 inhibition results in concomitant S3 inhibition (CD4$^{\Delta lg}$·N$^{\Delta E}$ lanes).

(Figure 4A). Of the inhibitors we tested, only 1,10 o-phenanthroline (OP), a divalent cation chelator commonly used as a broad-spectrum metalloprotease inhibitor, exhibited potent S2 inhibition. We observed equivalent decreases in NEXT and NICD production in the presence of OP (Figure 4). Importantly, OP did not inhibit S3 cleavage of N$^{\Delta E}$ directly (Figure 4B); therefore, the coincident reduction of S2 and S3 seen in Figure 4 supports the cascade model. This result implicates the metalloprotease family in S2 proteolysis and is consistent with the observation that TACE, a metalloprotease, can cleave Notch at Ala-1710 in vitro (Brou et al., 2000).

Do Kuzbanian or Presenilin Play a Role in S2 Processing?

Two genes have been implicated recently in Notch proteolysis, *kuzbanian* (*kuz*) and *presenilin1* (*PS1*). Both are believed to act upstream of Notch activation; N^{IC} proteins are epistatic to mutations in either gene (Sotillos et al., 1997; Wen et al., 1997; Levitan and Greenwald, 1998). PS1 has been implicated as the S3 protease or as an obligatory cofactor for S3 cleavage (De Strooper et al., 1999; Wolfe et al., 1999). To test whether PS1 plays a role in S2 cleavage, we compared the proteolytic profile of Notch constructs transfected into primary mouse embryonic fibroblasts (MEF) prepared from PS1-deficient embryos or wild-type embryos. Consistent with our previous results, NICD production is inhibited in PS1$^{-/-}$ cells; moreover, NEXT accumulates in these cells (Figure 5A). This finding demonstrates that the formation of a PS1/Notch complex, despite being required for efficient S3 cleavage (De Strooper et al., 1999; Ray et al., 1999a, 1999b), is not essential for S2 processing.

A possible candidate for the S2 protease is the ADAM family member Kuzbanian (Kuz, ADAM 10 in humans, sup-17 in *C. elegans*; Rooke et al., 1996; Sotillos et al., 1997; Wen et al., 1997), closely related to ADAM 17/TACE. Members of this family are known to be involved in the process of ectodomain shedding and are sensitive to 1,10 o-phenanthroline due to a dependence on zinc for activity (Turner and Hooper, 1999). To directly test the role of Kuz in Notch processing, we transfected MEF cells deficient for Kuz with activated Notch constructs. As shown in Figure 5B, all the processing events associated with N$^{LNR\ CC\rightarrow SS}$ occur in both Kuz$^{-/-}$ cells and Kuz$^{+/+}$ cells. Thus, although Kuz activity is genetically required cell autonomously in Notch-expressing cells (Rooke et al., 1996; Sotillos et al., 1997; Wen et al., 1997), Kuz is not required for S2 cleavage to occur. This result does not rule out the possibility that Kuz is among the enzymes capable of S2 cleavage in vivo since loss of TACE, capable of catalyzing S2 cleavage in vitro (Brou et al., 2000) does not result in a Notch phenotype in mice (Peschon et al., 1998).

Ligand Activation of Full-Length Notch Results in NEXT Production

For NEXT to be a true signaling intermediary, it should be regulated in a ligand-dependant manner. In order to demonstrate that S2 is relevant to activation of the full-length receptor, N^{FL6MT} constructs were cotransfected with CSL$^{RBP\text{-}J\kappa}$ and the DSL family member Jagged, as previously described (Schroeter et al., 1998). Western immunoblot analysis shows that NEXT and NICD both accumulate in the presence of Jagged (Figure 6A). This result demonstrates that S2 proteolysis occurs in response to ligand activation of the full-length Notch1 receptor. However, one caveat of this and previous cotransfection experiments stems from a question of whether Notch is activated by a ligand presented by the same cell (in *cis*) or from a neighboring cell (in *trans*). Classically, it is thought that the pathway is activated in *trans* and that *cis* interactions may in fact be antagonistic (Micchelli et al., 1997; Jacobsen et al., 1998). The cells used in our cotransfection assay (HEK 293T; Figure 6A) could allow either form of interaction to take place because they maintain an epithelial morphology with tight cell–cell contacts and transfect at very high efficiency. Coculture experiments, between Notch-expressing and ligand-expressing cells, have been conducted

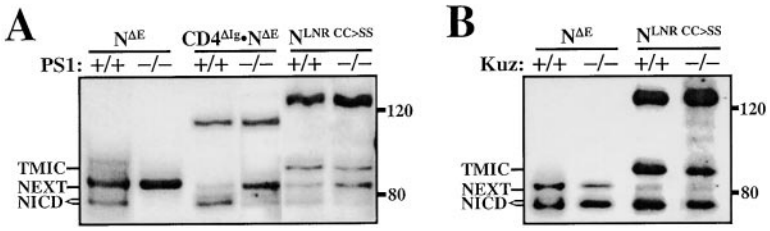

Figure 5. S2 Processing Occurs in Presenilin1- and Kuzbanian-Deficient Cells

(A) Mouse embryonic fibroblasts (MEFs) from PS1-deficient cells are competent for NEXT production. Anti-myc Western blot of cell lystaes is shown. SV40 immortalized MEF cells, derived from PS1$^{-/-}$ or wild-type embryos, were transfected with the indicated constructs. Cells were lysed 48 hr posttransfection. As previously demonstrated, PS1$^{-/-}$ MEFs show dramatically reduced NICD processing (De Strooper et al., 1999), which results in NEXT accumulation.

(B) MEFs from Kuz-deficient cells are competent for NEXT production. Anti-myc Western blot of cell lystaes is shown. SV40 immortalized MEF cells, derived from Kuz$^{-/-}$ or wild-type littermates, were transfected with the indicated constructs. Cells were lysed 48 hr posttransfection. S1, S2, and S3 cleavage products (TMIC, NEXT, and NICD) are all detected in both Kuz wild-type and Kuz-deficient cells.

measuring target gene activation and documenting effects on cellular differentiation, but no evidence was presented that ligand activation induced Notch proteolysis in these studies (Lindsell et al., 1995; Jarriault et al., 1998; Kuroda et al., 1999). It has been shown that coculture with Jagged2-expressing 3T3 cells results in novel cleavage of Notch1; however, the data presented could not discern whether the induced product(s) was NEXT, NICD, or both ("p115"; Luo et al., 1997). Therefore, in order to confirm that *trans* interactions at the cell surface between Notch and its ligands lead to NEXT and NICD production, HeLa cells expressing Notch and CSL$^{RBP\text{-}J\kappa}$ were cocultured with HEK 293T cells or HEK 293T expressing exogenous Jagged. Western blot analysis of cell lysates and CSL CO-IP verified that both S2 and S3 proteolysis are strongly induced when receptor–ligand interactions occur exclusively in *trans* (Figure 6B). This result provides further support to the hypothesis that the S2 cleavage occurs extracellularly at the plasma membrane. Note also that HEK 293T cells alone can induce a low level of S2 and S3 cleavage when presented in *trans* at confluence. We attribute this to a low level of endogenous expression of ligands in these cells (J. S. M. and R. K., unpublished data). Taken together, these results support the hypothesis that ligand binding serves to relieve extracellular inhibition of S3 cleavage by promoting S2 cleavage. This ectodomain shedding–like process creates NEXT, a N$^{\Delta E}$-like molecule, which undergoes S3 cleavage, producing NICD and leading to Notch activation.

Discussion

Precise details of the molecular events leading to Notch activation have only recently begun to be elucidated. Truncated, membrane-tethered, activated Notch proteins undergo ligand-independent proteolytic processing, resulting in release of NICD and its nuclear translocation (Jarriault et al., 1995; Kopan et al., 1996; Schroeter et al., 1998; Struhl and Adachi, 1998). This cleavage is mediated by a presenilin-containing complex (De Strooper et al., 1999; Struhl and Greenwald, 1999; Ye et al., 1999) and occurs within the transmembrane domain (J. S. M. and R. K., unpublished data). While the cell surface Notch receptor is found in a complex containing PS1 (Ray et al., 1999b), no S3 cleavage is observed in the absence of ligand (Schroeter et al., 1998). To gain insight into the regulatory mechanism preventing intramembranous cleavage of Notch1, we used a predominantly biochemical approach to investigate what molecular differences exist between several classes of activated and inactive Notch protein. Our analysis reveals that Notch signaling is activated by an extracellular processing event that serves to relieve inhibition of the intramembranous cleavage.

S2: A Ligand-Induced Extracellular Proteolytic Event

Inspired by a structure-function analysis of *Drosophila* Notch (Lieber et al., 1993) and by chimeric fusion protein studies, we have generated ligand-independent activated Notch proteins as substrates for biochemical analysis. N$^{LNR\ CC\rightarrow SS}$ retains the putative extracellular negative control region, while CD4·Notch proteins contain a heterologous ectodomain. We find that a common feature of activated Notch proteins and the full-length receptor responding to ligand binding is that all are cleaved at a novel proteolytic site, S2 (Figures 1, 2, and 6). N-terminal sequencing of the membrane associated product, NEXT, determined that S2 cleavage occurs at an extracellular site, between residues Ala-1710 and Val-1711, approximately 12 amino acids outside the transmembrane domain. To date, the S2 cleavage product has only been successfully sequenced from the active CD4·Notch fusion protein. Therefore, we cannot rule out slight shifts of 2–3 amino acids in other contexts. However, Brou and colleagues have identified the same site independently and provided evidence that the sheddase TACE can mediate S2 cleavage.

A Proteolytic Cascade Activates Notch

Inhibition of S2 by metalloprotease inhibitors (Figure 4) results in loss of S3 cleavage. Conversely, blocking S3 cleavage by mutation, multiple protease inhibitors, or loss of PS1 leads to the accumulation of NEXT (Figures 3B, 3C, and 5A). In addition, pulse-chase analysis has previously shown that the NEXT-like N$^{\Delta E}$ is completely converted into NICD (Schroeter et al., 1998). While we cannot rule out that under some unidentified circumstances Notch may be directly processed at S3, NEXT appears to be the only direct precursor of NICD. These results suggest that Notch is regulated by a sequential series of at least two proteolytic events. Interestingly, both types of truncated, constitutively active Notch proteins imitate naturally occurring proteolytic products of Notch signaling; N$^{\Delta E}$ constructs mimic NEXT, and N^{IC} constructs mimic NICD.

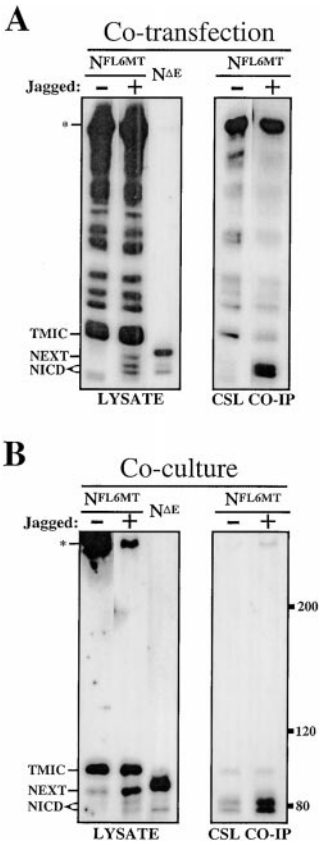

Figure 6. Ligand Induction of S2 Processing

(A) Ligand activation of the Notch1 receptor results in induction of S2 processing. Anti-myc Western blot of anti-Flag coimmunoprecipitation (CSL CO-IP) and corresponding cell extract (LYSATE) is shown. HEK 293T cells were cotransfected with N^{FL6MT} and $CSL^{RBP\text{-}J\kappa}$, with or without Jagged. Cells were lysed in coimmunoprecipitation buffer 48 hr posttransfection. Ligand-induced S2 cleavage is clearly evident in lysates from cells cotransfected with Jagged. As previously demonstrated, cotransfection with ligand induces S3 cleavage, which can be enriched by CSL CO-IP (Schroeter et al., 1998). Note that NICD appears as a doublet at this resolution, the upper band is a posttranslational modification of NICD of unknown significance (Schroeter et al., 1998).

(B) S2 proteolysis is induced by interactions between cells (in *trans*), suggesting NEXT is produced at the plasma membrane or upon internalization. Anti-myc Western blot of anti-Flag coimmunoprecipitation (CSL CO-IP) and corresponding cell extract (LYSATE) is shown. HeLa cells, cotransfected with N^{FL6MT} and $CSL^{RBP\text{-}J\kappa}$, were cocultured with a confluent layer of HEK 293T cells or HEK 293T cells transfected with Jagged; 36 hr posttransfection, controls and Jagged transfected cells were gently resuspended by repeated rinsing and plated over $N^{FL6MT}/CSL^{RBP\text{-}J\kappa}$ transfected HeLa cells. Plates were spun at 1000 rpm for 5 min and returned to incubator. Cocultures were lysed in coimmunoprecipitation buffer 4 hr later. Coculturing in the presence of exogenous ligand produced a robust induction of both S2 and S3 cleavage products. Note also a minimal induction of S2 and S3 in the control condition. We attribute this to the endogenous expression of ligands at low levels in these cells (J. S. M. and R. K., unpublished data).

Regulation of Notch processing is complex. Full-length Notch proteins are not converted to NICD without ligand binding (Figure 6), while for $N^{\Delta E}$ S3 can proceed even in the presence of S2 inhibitors (Figure 4B and Brou et al., 2000). It has been observed that longer $N^{\Delta E}$ constructs, containing the conserved cysteines, are active without obvious NICD production (Aster et al., 1994; Pear et al., 1996). Consistent with this, we observe low but consistent levels of Notch processing and Hes1 activation from N^{LNR} (Schroeter et al., 1998; Figure 1) but not from full-length Notch. One possible explanation is that a correlation exists between ectodomain length, or structure, and S3 processing efficiency; S3 cleavage being most efficient only in molecules with short extramembranous domains or with a permissive structure, such as $CD4^{\Delta Ig}.N^{\Delta E}$, while longer proteins become increasingly dependent on S2 cleavage to remove the inhibitory juxtamembrane region. Interestingly, it has recently been demonstrated that calcium depletion results in dissociation of the extracellular domain and subsequent activation of Notch (Rand et al., 2000). Thus, ectodomain repression is dependent on the post-S1 heterodimeric bond between Notch termini, and EDTA-mediated shedding of the extracellular domain is sufficient for activation. While this is not a concern with $CD4^{\Delta Ig}.N^{\Delta E}$, $N^{LNR\ CC\rightarrow SS}$ maintains the heterodimeric bond and, therefore, it is not activated by this mechanism (Figures 1D and 1E). S2 cleavage occurs constitutively in $N^{LNR\ CC\rightarrow SS}$ and $CD4^{\Delta Ig}.N^{\Delta E}$; however, in full-length Notch, S2 cleavage is regulated by the conformation of the domain amino-terminal to it, requiring ligand binding for processing. Ligand binding must therefore cause a conformational change that promotes S2 proteolysis. A requirement for dynamin (Seugnet et al., 1997) and endocytosis (Parks et al., 2000) for Notch signaling suggests that a possible stress-induced conformational change is involved in exposing S2 to proteolysis. The resultant polypeptide (NEXT) undergoes constitutive S3 cleavage if occuring in an S3-competent cellular compartment (e.g., the plasma membrane). It should be noted that when Notch is expressed at high levels, NEXT accumulation without efficient conversion to NICD has been observed (J. S. M. and R. K., unpublished data). It is possible that high protein density at the cell surface may inhibit S3 proteolysis, and this possibility is under further investigation.

While a more extensive structure-function analysis will be required to reveal the molecular mechanism responsible for protease resistance in the absence of ligand binding, it appears that Notch, SREBP, and APP are regulated by similar proteolytic cascades (Figure 7B). Like Notch, SREBP is regulated by ligand-initiated extracellular cleavage followed by a second, activating cleavage occurring near the outer margin of the transmembrane domain (Brown and Goldstein, 1997). APP is also thought to undergo sequential processing: release of the APP extramembranous domain, by β- or α-secretase activity, being required prior to γ-secretase processing (Mills and Reiner, 1999). Thus, a general feature of proteins that undergo intramembranous proteolysis appears to be cleavage of their ectodomain prior to intramembranous cleavage. This seems to be the case without apparent structural similarity of the proteins or cleaving enzymes (Notch and APP are cleaved by γ-secretase[s], SREBP by the unrelated S2 protease). Our results uphold previous speculations (Chan and Jan, 1998, 1999; Hardy and Israël, 1999) linking the three proteins in one mechanistic paradigm.

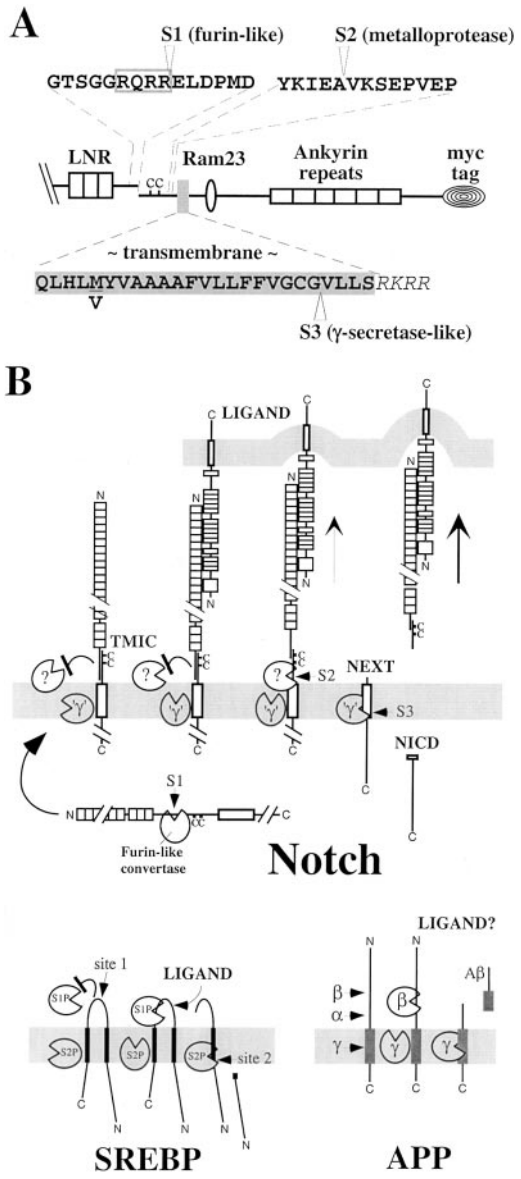

Figure 7. Model

(A) The S1, S2, and S3 cleavage sites (arrowheads) are indicated above amino acid sequences. The boxed region before S1 indicates the furin recognition site; this information is not yet available for γ-secretase or the S2 metalloprotease. Met-1727 has been mutated to Val (M/V) in the $N^{\Delta E}$ construct to circumvent aberrant translation initiation (Kopan et al., 1996).

(B) Diagram depicting elements of a shared proteolytic regulatory mechanism between Notch, APP, and SREBP. All three proteins require extracellular processing in order to allow a subsequent intramembranous proteolysis. Notch and SREBP are activated via a similar proteolytic cascade. Initially, Notch and SREBP are protease resistant. Both undergo ligand-induced proteolysis; ligand binding is postulated to cause a conformational change (or changes) in the ectodomain that exposes the extracellular/luminal cleavage site to protease activity. The Notch extracellular domain may be internalized into the ligand-expressing cell ("shed"; Parks et al., 2000). The carboxy-terminal product of this step (NEXT and its SREBP equivalent) undergoes a second intramembranous proteolytic step. The final product (NICD and its SREBP equivalent) enters the nucleus and ultimately activates transcription, SREBP directly and Notch via association with CSL. Notch and APP share an overall proteolytic profile and are processed at their respective intramembranous site

Metalloproteases, Notch, and Ectodomain Shedding

Genetic analyses have implicated Kuz (ADAM 10, SUP17) in Notch signaling (Rooke et al., 1996; Pan and Rubin, 1997; Sotillos et al., 1997; Wen et al., 1997). Although an initial inhibitor screen strongly implicates the metalloprotease family in S2 cleavage, our findings suggest that Kuz cannot be the sole S2 protease (Figure 5B). This is consistent with recent findings that suggest that Kuz cleaves the Notch ligand Delta but not the receptor itself (Qi et al., 1999) and that TACE is capable of cleaving Notch at Ala-1710 (Brou et al., 2000). Striking similarities in the phenotypes of $Notch1^{-/-}$ and $Kuz^{-/-}$ mice (Pan et al., submitted), however, underscore the intimate link between these molecules.

TACE is among a number of enzymes (termed alternatively secretases or sheddases) known to mediate a proteolytic process termed ectodomain shedding, whereby transmembrane proteins are cleaved extracellularly and released into the extracellular milieu (Kiessling and Gordon, 1998). Ectodomain shedding is known to play key roles in cancer invasion, metastasis, activation of soluble ligands, and protein turnover. Sheddases generally exhibit low substrate specificity, and some are believed to be more dependent on structural motifs than primary residues, often cleaving at a fixed distance from the transmembrane domain (e.g., TACE). Disruption of the TACE locus in mice unexpectedly results in embryonic lethality, implicating TACE and ectodomain shedding in essential developmental events and suggesting TACE normally cleaves substrates other than pro-TNFα (Peschon et al., 1998). While no direct evidence is presented here that S2 cleavage results in shedding of Notch per se, recent reports demonstrated that dissociation of the extracellular domain is sufficient for activation (Rand et al., 2000). Further, it has been observed that the extracellular domain of Notch alone is *trans*-endocytosed (thus "shed") into ligand-expressing cells when Notch is activated during pupal wing vein and retinal pigment cell development in *Drosophila* (Parks et al., 2000). If correct, this model would predict that truly "soluble" ligands will fail to activate Notch, but membrane-tethered or extracellular matrix associated ligands will.

A final consideration must be taken into account concerning the involvement of metalloprotease(s) in Notch activation. Notch pathway activation has been shown to serve as a secondary event contributing to the oncogenic transformation of either Myc- (Girard et al., 1996) or E1A- (Capobianco et al., 1997) expressing cells. Elevated metalloprotease activity, which is often linked to transformation and metastasis, may lead to ectopic, ligand-independent activation of the endogenous Notch receptor. This may explain why nuclear Notch staining is often found in various tumors (Zagouras et al., 1995)

by related but unidentified proteases, "γ-secretase(s)." Similar parallels between α- or β-secretase and extracellular processing of Notch are possible; however, further experimentation and identification of the proteases responsible for these cleavage events will be required. In retrospect, it is not surprising that activated Notch proteins described to date mimic or facilitate the production of NEXT and NICD.

and suggests that ectopic, metalloprotease-mediated Notch activation may be a common event during oncogenesis.

Experimental Procedures

Plasmid Constructions

All Notch1 and CD4·N1 fusion constructs reported here were cloned into the pCS2+MT vector (Rupp et al., 1994; Turner and Weintraub, 1994) and have the C-terminal 348 residues (Leu-2192 to C terminus) of Notch replaced with a hexameric myc tag to facilitate biochemical analysis. Hes1-Luciferase, wild type, and V1744K Notch1 constructs, ΔE (M1727V), LNR, and FL, have been previously described (Jarriault et al., 1995; Kopan et al., 1996; Schroeter et al., 1998). PCR mutagenesis was used to create the C1675S and C1682S mutations and HA N-terminally tagged versions of LNR. Fusions between the extracellular domain of human CD4 and mouse Notch1 ΔE (M1727V) were constructed as shown in Figure 2A. Briefly, a full-length (CD4, amino acids 1–352) or truncated ($CD4^{\Delta Ig}$, amino acids 1–201) CD4 ectodomain was fused to the N terminus of $N^{\Delta E}$ (Ile-1704) to create two chimeric constructs, $CD4{\cdot}N^{\Delta E}$ and $CD4^{\Delta Ig}{\cdot}N^{\Delta E}$, respectively. All constructs were sequenced to confirm mutation. Complete details of all cloning procedures are available upon request.

Cell Culture, Transfections, and Reporter Assays

Cells were grown in DMEM supplemented with 2 mM glutamine, 100 μg/ml each penicillin and streptomycin, and either 10% bovine calf serum (NIH 3T3) or 10% fetal bovine serum (HEK 293T, HeLa, and MEF) and incubated at 37°C in an atmosphere of 5% CO_2. Cells were transfected using a modified $Ca^{2+}PO_4$ precipitation technique (Chen and Okayama, 1987). The Hes1-Luciferase reporter assay was performed as described previously (Jarriault et al., 1995; Schroeter et al., 1998). Briefly, a mixture of DNAs containing 0.1 μg/ml of Notch expression plasmids, 0.5 μg/ml Hes1-Luc, and 0.01 mg/ml of pCS2+ β-gal was transfected into 3T3 cells (pCS2+ added to final concentration of 1 μg/ml). Luciferase activity was normalized to β-gal expression levels to control for transfection efficiency. Cells were lysed and luminescence assessed 48 hr posttransfection.

Immunoprecipitation, Coimmunoprecipitation, SDS-PAGE, and Western Blotting

All cells were lysed and processed 48 hr posttransfection. All protein samples were resolved by 6% SDS-PAGE after boiling 5 min in SDS-PAGE sample buffer (Laemmeli buffer). For Western blot analysis, proteins were transferred to nitrocellulose in Tris-glycine-methanol buffer and visualized with 9E10 anti-myc hybridoma supernatant followed by HRP-conjugated anti-mouse secondary antibody (Amersham, Pharmacia, Uppsala, Sweden) and ECL luminescent substrate detection (Pierce, Rockford, IL). Cells were lysed in 1 ml of boiling 5× Lammeli buffer. Samples were then passed through a 26 gauge needle repeatedly and spun down to remove debris. For immunoprecipitations (IP), cells were lysed for 5 min in 300 μl boiling TN buffer (50 mM Tris [pH 7.4], 100 mM NaCl), containing 1% SDS and proteinase inhibitors (0.5 μg/ml aprotinin, 0.5 μg/ml leupeptin, 0.2 mM PMSF, and 5 mM 1,10 o-phenanthroline) and processed as above. The supernatant was diluted 1:4 into TN containing 1% Triton X-100, 0.5% deoxycholate, 1% bovine serum albumin, and proteinase inhibitors as above, with 50 μl protein A-Sepharose CL-4B (Sigma, St. Louis, MI) and 1 μg/ml of the appropriate antibody: 9E10 anti-myc monoclonal (Sigma), HA.11 anti-HA polyclonal (BAbCo, Richmond, CA). IP supernatants were mixed overnight at 4°C followed by rinsing four times in the diluent above and twice with TN. The supernatant was completely removed, and beads were resuspended in Laemmeli buffer. $CSL^{RBP\text{-}J\kappa}$ coimmunoprecipitation (CSL CO-IP) was performed with M2 anti-Flag agarose (Sigma) as described (Schroeter et al., 1998). LYSATE samples (50 μl) were removed from CO-IP and IP supernatant and diluted 1:1 with 2× Laemmeli buffer prior to precipitation. For biotinylation, cells were labeled with Sulfo-EGS-Biotin (Pierce) as described in manufacturer's protocol. Biotinylated proteins were then immunoprecipitated with agarose streptavidin as above (Vector, Burlingame, CA). In some figures, different exposures of the same gels were spliced to produce images with equivalent exposure using Canvas 6 (Deneba, Miami, FL) software.

S2 Sequencing, Drug Treatments, and Metabolic Labeling

For N-terminal sequencing of NEXT, 20 100 mm dishes of HEK 293T cells were transfected with 2 μg of $CD4^{\Delta Ig}{\cdot}N^{\Delta E}$ V→K each. Cells were treated with 50 μM calpeptin to stabilize the polypeptide 8 hr, and again 4 hr, prior to lysis. Cells were lysed 48 hr after transfection, pooled, and immunoprecipitated with 9E10 anti-myc as above. Following immunoprecipitation, proteins were resolved by 6% SDS-PAGE and transferred to PVDF membrane in CAPS buffer. Proteins were visualized with Commassie blue, and the band corresponding to NEXT was excised and subjected to N-terminal sequencing on an ABI model 473 sequencer. For inhibitor studies, cells were labeled with 50 μCi/ml ^{35}S in the presence of the indicated reagent for 4 hr prior to lysis. Notch proteins were then anti-myc immunoprecipitated and resolved by 6% SDS-PAGE. Gels were dried and visualized by autoradiography. Quantification of band intensity was performed using a Molecular Dynamics phosphoimager and ImageQuant software.

Acknowledgments

We wish to thank Drs. Bart De Strooper and Paul Saftig for kindly providing $PS1^{-/-}$ cells; Drs. Alain Israël, Marc Muskavitch, and Spyros Artavanis-Tsakonas for communicating results prior to publication; Drs. Tom Broekelmann and Robert Mecham for amino acid sequencing, and Jeffrey A. Kisslinger for technical support. We also wish to thank Drs. Ross Cagan, Irving Boime, Alison Goate, Keith Blackwell, and Jeffrey Gordon for comments on the manuscript and members of the Kopan lab for insightful discussions during the course of this project. J. S. M. was supported in part as a Lucille P. Markey Pathway predoctoral fellow. J. S. M., E. H. S., M. T. S., X. T., and R. K. are supported by NIH grant GM 55479.

Received August 13, 1999; revised January 4, 2000.

References

Aster, J., Pear, W., Hasserjian, R., Erba, H., Davi, F., Luo, B., Scott, M., Baltimore, D., and Sklar, J. (1994). Functional analysis of the TAN-1 gene, a human homolog of *Drosophila* Notch. Cold Spring Harbor Symp. Quant. Biol. *LIX*, 125–136.

Blaumueller, C.M., Qi, H.L., Zagouras, P., and Artavanis-Tsakonas, S. (1997). Intracellular cleavage of Notch leads to a heterodimeric receptor on the plasma membrane. Cell *90*, 281–291.

Brou, C., Logeat, F., Gupta, N., Bessia, C., LeBail, O., Doedens, J.R., Cumano, A., Roux, P., Black, R., and Israël, A. (2000). A novel proteolytic cleavage involved in Notch signaling: the role of the disintegrin-metalloprotease TACE. Mol. Cell *5*, this issue, 207–216.

Brown, M.S., and Goldstein, J.L. (1997). The SREBP pathway—regulation of cholesterol metabolism by proteolysis of a membrane-bound transcription factor. Cell *89*, 331–340.

Capobianco, A.J., Zagouras, P., Blaumueller, C.M., Artavanistsakonas, S., and Bishop, J.M. (1997). Neoplastic transformation by truncated alleles of human Notch1/Tan1 and Notch2. Mol. Cell. Biol. *17*, 6265–6273.

Chan, Y.M., and Jan, Y.N. (1998). Roles for proteolysis and trafficking in Notch maturation and signal transduction. Cell *94*, 423–426.

Chan, Y.M., and Jan, Y.N. (1999). Presenilins, processing of β-amyloid precursor protein, and Notch signaling. Neuron *23*, 201–204.

Chen, C., and Okayama, H. (1987). High efficiency transformation of mammalian cells by plasmid DNA. Mol. Cell. Biol. *7*, 2745–2752.

De Strooper, B., Annaert, W., Cupers, P., Saftig, P., Craessaerts, K., Mumm, J.S., Schroeter, E.H., Schrijvers, V., Wolfe, M.S., Ray, W.J., et al. (1999). A presenilin-1-dependent gamma-secretase-like protease mediates release of Notch intracellular domain. Nature *398*, 518–522.

Greenwald, I. (1994). Structure/function studies of lin-12/Notch proteins. Curr. Opin. Genet. Dev. *4*, 556–562.

Greenwald, I. (1998). Lin-12/Notch signalinγ—lessons from worms and flies. Genes Dev. *12*, 1751–1762.

Girard, L., Hanna, Z., Beaulieu, N., Hoemann, C.D., Simard, C., Kozak, C.A., and Jolicoeur, P. (1996). Frequent provirus insertional mutagenesis of Notch1 in thymomas of Mmtv(D)/Myc transgenic mice suggests a collaboration Of C-Myc and Notch1 for oncogenesis. Genes Dev. *10*, 1930–1944.

Gridley, T. (1997). Notch signaling in vertebrate development and disease. Mol. Cell. Neurosci. *9*, 103–108.

Hardy, J., and Israël, A. (1999). Alzheimer's disease—in search of gamma-secretase. Nature *398*, 466–467.

Jacobsen, T.L., Brennan, K., Martinez Arias, A., and Muskavitch, M.A.T. (1998). Cis-interactions between Delta and Notch modulate neurogenic signaling in *Drosophila*. Development *125*, 4531–4540.

Jarriault, S., Brou, C., Logeat, F., Schroeter, E.H., Kopan, R., and Israël, A. (1995). Signalling downstream of activated mammalian Notch. Nature *377*, 355–358.

Jarriault, S., Lebail, O., Hirsinger, E., Pourquie, O., Logeat, F., Strong, C.F., Brou, C., Seidah, N.G., and Israël, A. (1998). Delta-1 activation of Notch-1 signaling results in Hes-1 transactivation. Mol. Cell. Biol. *18*, 7423–7431.

Kiessling, L.L., and Gordon, E.J. (1998). Transforming the cell surface through proteolysis. Chem. Biol. *5*, R49–R62.

Kimble, J., Henderson, S., and Crittenden, S. (1998). Notch/Lin-12 signaling—transduction by regulated protein slicing. Trends Biochem. Sci. *23*, 353–357.

Kopan, R., Schroeter, E.H., Weintraub, H., and Nye, J.S. (1996). Signal transduction by activated mNotch: importance of proteolytic processing and its regulation by the extracellular domain. Proc. Natl. Acad. Sci. USA *93*, 1683–1688.

Kuroda, K., Tani, S., Tamura, K., Minoguchi, S., Kurooka, H., and Honjo, T. (1999). Delta-induced notch signaling mediated by RBP-J inhibits MyoD expression and myogenesis. J. Biol. Chem. *274*, 7238–7244.

Levitan, D., and Greenwald, I. (1998). Effects of SEL-12 presenilin on LIN-12 localization and function in *Caenorhabditis elegans*. Development *125*, 3599–3606.

Lewis, J. (1998). Notch signaling and the control of cell fate choices in vertebrates. Semin. Cell Dev. Biol. *9*, 583–589.

Lieber, T., Kidd, S., Alcamo, E., Corbin, V., and Young, M.W. (1993). Antineurogenic phenotypes induced by truncated Notch proteins indicate a role in signal transduction and may point to a novel function for Notch in nuclei. Genes Dev. *7*, 1949–1965.

Lindsell, C.E., Shawber, C.J., Boulter, J., and Weinmaster, G. (1995). Jagged: a mammalian ligand that activates Notch1. Cell *80*, 909–917.

Logeat, F., Bessia, C., Brou, C., Lebail, O., Jarriault, S., Seidah, N.G., and Israël, A. (1998). The Notch1 receptor is cleaved constitutively by a furin-like convertase. Proc. Natl. Acad. Sci. USA *95*, 8108–8112.

Luo, B., Aster, J.C., Hasserjian, R.P., Kuo, F., and Sklar, J. (1997). Isolation and functional analysis of a cDNA for human Jagged2, a gene encoding a ligand for the Notch1 receptor. Mol. Cell. Biol. *17*, 6057–6067.

Micchelli, C.A., Rulifson, E.J., and Blair, S.S. (1997). The function and regulation of cut expression on the wing margin of *Drosophila*—Notch, Wingless and a dominant negative role for Delta and Serrate. Development *124*, 1485–1495.

Mills, J., and Reiner, P.B. (1999). Regulation of amyloid precursor protein cleavage. J. Neurochem. *72*, 443–460.

Pan, D.J., and Rubin, G.M. (1997). Kuzbanian controls proteolytic processing of Notch and mediates lateral inhibition during Drosophila and vertebrate neurogenesis. Cell *90*, 271–280.

Parks, A.L., Klueg, K.M., Stout, J.R., and Muskavitch, M.A.T. (2000). Ligand endocytosis drives receptor dissociation and activation in the Notch pathway. Development *127*, in press.

Pear, W.S., Aster, J.C., Scott, M.L., Hasserjian, R.P., Soffer, B., Sklar, J., and Baltimore, D. (1996). Exclusive development of T cell neoplasms in mice transplanted with bone marrow expressing activated Notch alleles. J. Exp. Med. *183*, 2283–2291.

Peschon, J.J., Slack, J.L., Reddy, P., Stocking, K.L., Sunnarborg, S.W., Lee, D.C., Russell, W.E., Castner, B.J., Johnson, R.S., Fitzner, J.N., et al. (1998). An essential role for ectodomain shedding in mammalian development. Science *282*, 1281–1284.

Qi, H.L., Rand, M.D., Wu, X.H., Sestan, N., Wang, W.Y., Rakic, P., Xu, T., and Artavanis-Tsakonas, S. (1999). Processing of the Notch ligand delta by the metalloprotease kuzbanian. Science *283*, 91–94.

Rand, M.D., Grimm, L.M., Artavanis-Tsakonas, S., Patriub, V., Blacklow, S.C., Sklar, J., Aster, J.C. (2000). Calcium depletion dissociates and activates heterodimeric Notch receptors. Mol. Cell. Biol. *20*, in press.

Ray, W.J., Yao, M., Nowotny, P., Mumm, J., Zhang, W., Wu, J.Y., Kopan, R., and Goate, A.M. (1999a). Evidence for a physical interaction between presenilin and Notch. Proc. Natl. Acad. Sci. USA *96*, 3263–3268.

Ray, W.J., Yao, M., Mumm, J., Schroeter, E.H., Saftig, P., Wolfe, M., Selkoe, D.J., Kopan, R., and Goate, A.M. (1999b). Cell surface presenilin-1 participates in the gamma-secretase-like cleavage of Notch1. J. Biol. Chem. *274*, 36801–36807.

Rooke, J., Pan, D., Xu, T., and Rubin, G.M. (1996). Kuz, a conserved metalloprotease-disintegrin protein with two roles in *Drosophila* neurogenesis. Science *273*, 1227–1231.

Rupp, R.A.W., Snider, L., and Weintraub, H. (1994). *Xenopus* embryos regulate the nuclear localization of XMyoD. Genes Dev. *8*, 1311–1323.

Sadhukhan, R., Sen, G.C., Ramchandran, R., and Sen, I. (1998). The distal ectodomain of angiotensin-converting enzyme regulates its cleavage-secretion from the cell surface. Proc. Natl. Acad. Sci. USA *95*, 138–143.

Sakihama, T., Smolyar, A., and Reinherz, E. (1995). Oligomerization of CD4 is required for stable binding to class II major histocompatibility complex proteins but not for interaction with human immunodeficiency virus gp120. Proc. Natl. Acad. Sci. USA *92*, 6444–6448.

Schroeter, E.H., Kisslinger, J.A., and Kopan, R. (1998). Notch-1 signaling requires ligand-induced proteolytic release of intracellular domain. Nature *393*, 382–386.

Seugnet, L., Simpson, P., and Haenlin, M. (1997). Requirement For dynamin during Notch signaling in *Drosophila* neurogenesis. Dev. Biol. *192*, 585–598.

Sotillos, S., Roch, F., and Campuzano, S. (1997). The metalloprotease-disintegrin Kuzbanian participates in Notch activation during growth and patterning of *Drosophila* imaginal discs. Development *124*, 4769–4779.

Struhl, G., and Adachi, A. (1998). Nuclear access and action of Notch in vivo. Cell *93*, 649–660.

Struhl, G., and Greenwald, I. (1999). Presenilin is required for activity and nuclear access of Notch in Drosophila. Nature *398*, 522–525.

Turner, A.J., and Hooper, N.M. (1999). Role for ADAM-family proteinases as membrane protein secretases. Biochem. Soc. Trans. *27*, 255–259.

Turner, D.L., and Weintraub, H. (1994). Expression of achaete-scute homolog 3 in *Xenopus* embryos converts ectodermal cells to a neural fate. Genes Dev. *8*, 1434–1447.

Weinmaster, G. (1997). The ins and outs of notch signaling. Mol. Cell. Neurosci. *9*, 91–102.

Wen, C.H., Metzstein, M.M., and Greenwald, I. (1997). Sup-17, a *Caenorhabditis Elegans* Adam protein related to *Drosophila* Kuzbanian, and its role in Lin-12/Notch signalling. Development *124*, 4759–4767.

Wolfe, M.S., Xia, W., Moore, C.L., Leatherwood, D.D., Ostaszewski, B., Rahmati, T., Donkor, I.O., and Selkoe, D.J. (1999). Peptidomimetic probes and molecular modeling suggest that Alzheimer's gamma-secretase is an intramembrane-cleaving aspartyl protease. Biochemistry *38*, 4720–4727.

Ye, Y.H., Lukinova, N., and Fortini, M.E. (1999). Neurogenic phenotypes and altered Notch processing in *Drosophila* Presenilin mutants. Nature *398*, 525–529.

Zagouras, P., Stifani, S., Blaumueller, C.M., Carcangiu, M.L., and Artavanis, T.S. (1995). Alterations in Notch signaling in neoplastic lesions of the human cervix. Proc. Natl. Acad. Sci. USA *92*, 6414–6418.